Metal Organic Frameworks as Nitric Oxide Catalysts

Jacqueline L. Harding[†] and Melissa M. Reynolds*[,†,‡]

[†]Department of Chemistry and [‡]School of Biomedical Engineering, Colorado State University, Fort Collins, Colorado, 80523

S *Supporting Information*

ABSTRACT: The use of metal organic frameworks (MOFs) for the catalytic production of nitric oxide (NO) is reported. In this account we demonstrate the use of $Cu_3(BTC)_2$ as a catalyst for the generation of NO from the biologically occurring substrate, S-nitrosocysteine (CysNO). The MOF catalyst was evaluated as an NO generator by monitoring the evolution of NO in real time via chemiluminescence. The addition of 2, 10, and 15-fold excess CysNO to MOF-Cu^{II} sites and cysteine (CysH) resulted in catalytic turnover of the active sites and nearly 100% theoretical yield of the NO product. Control experiments without the MOF present did not yield appreciable NO generation. In separate studies the MOF was found to be reusable over successive iterations of CysNO additions without loss of activity. Subsequently, the MOF catalyst was confirmed to remain structurally intact by pXRD and ATR-IR following reaction with CysNO and CysH.

Nitric oxide (NO) has been identified as a crucial biological signaling molecule in the cardiovascular,[1−3] nervous, and immune systems.[1,4−6] As a result, NO storage and delivery vehicles have been extensively developed to target a range of diseases and to control material−cell interactions.[2] Current approaches for NO storage and delivery have primarily focused on incorporating NO donor moieties such as diazeniumdiolates ($R-N_2O_2$) and S-nitrosothiols (RSNO) onto both organic[3] and inorganic[4] substrates. However, the relatively small NO reservoir that can be stored on such donor substrates ultimately limits their potential use.

In order to increase the NO loading capacity and expand the potential use of NO donor materials to more diverse biomedical applications, porous inorganic materials such as metal organic frameworks (MOFs) and zeolites have been investigated as NO storage materials. MOF materials provide an NO therapeutic substrate with tunable physical and chemical properties.[5] Recently, the Morris, Rosseinsky, and Cohen groups have postsynthetically modified MOFs with various NO donor moieties.[6] Their work shows that MOF substrates are[7] indeed viable NO donor materials. These NO donor MOF materials have increased storage capacity over previous NO donors.

Yet, even the use of a MOF substrate does not eliminate the capacity and NO-release duration limitations that are inherent in NO donor materials. Long-term biomedical applications require a therapeutic substrate that is stable and capable of producing NO for lengthy and sustained periods of time. Advantageously, structured inorganic materials such as zeolites and MOFs offer the potential to be either NO donors or catalysts for the generation of NO directly from bioavailable sources. Recently, the Morris group has demonstrated that Cu-based zeolites can be used to catalytically produce NO from nitrite and to store NO. Thus, MOFs and zeolites offer a single therapeutic substrate that can be designed as either an NO donor or an NO generator.

While there are numerous bioavailable sources of NO, including nitrite (176 nM) and S-nitrosothiols (RSNOs) (10 μM), the most abundant and structurally varied species in the blood are RSNOs. As such, RSNO decomposition has been the most heavily investigated. RSNOs have been reported to decompose via several different mechanisms.[7] One well-established mechanism of RSNO decomposition involves a copper-mediated pathway with thiol reducing equivalents resulting in the generation of 1 mol of NO and the corresponding disulfide.[7] MOFs have been previously demonstrated to catalyze a variety of reactions. Thus, we propose that MOFs can be utilized as catalysts for long-term NO generation by selectively permitting the diffusion of RSNO substrates to the active Cu^{II} sites.

The general requirements for a MOF−NO catalyst are that the material is resistant to degradation under the reaction conditions and has accessible catalytic sites. To this end, three MOFs were investigated: $Cu_3(BTC)_2$ (BTC:1,3,5-benzenetricarboxylate), Cu-triazolate, and Fe(BDC) (BDC-benzenedicarboxylate). Of these, only $Cu_3(BTC)_2$ met the specified requirements. $Cu_3(BTC)_2$ features unsaturated metal sites and pore sizes up to 18 Å that allow for the accessibility of the RSNO species to the metal center.[8] In addition, previous reports have demonstrated that $Cu_3(BTC)_2$ remains structurally stable after being utilized as a catalyst for other reactions.[9] Thus, this well-studied MOF presents an ideal starting point for studying the catalytic production of NO via the copper-mediated decomposition of RSNOs. In this work, we report the first example of using a MOF to catalyze the decomposition of RSNOs to generate NO.

As depicted in Figure 1, RSNOs can interact with the Cu^{II} metal sites of $Cu_3(BTC)_2$ to decompose RSNO and subsequently produce NO. The RSNO decomposition reaction to generate NO via the $Cu_3(BTC)_2$ catalyst is shown in Scheme 1. S-Nitrosocysteine (CysNO) was selected as a model RSNO species because of its reported bioavailability in the micromolar range.[10] In addition, these RSNOs do not decompose prematurely with reducing equivalents of cysteine (CysH) to a significant extent (see Table 1). Both reactions were monitored by measuring the formation of the product, NO.
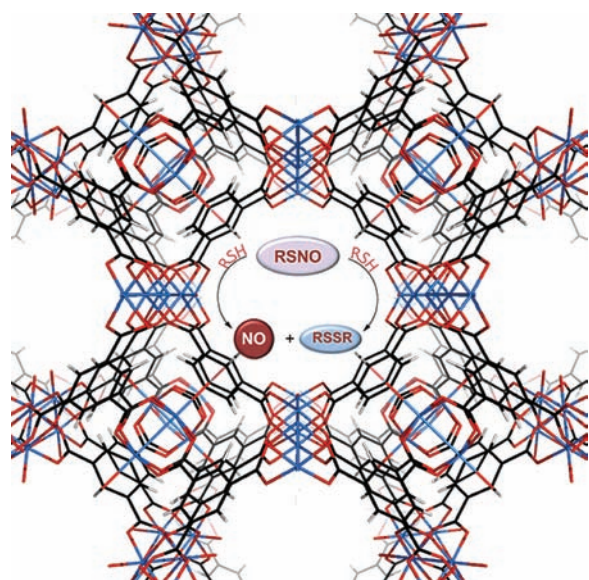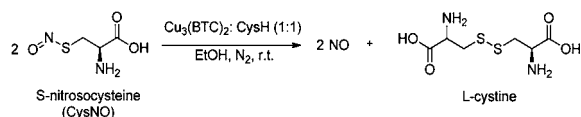
Figure 1. Schematic illustration of RSNO decomposition to produce NO via a MOF catalyst: $Cu_3(BTC)_2$; copper sites are shown in blue, the oxygen sites in red, and the BTC ligand in black.

Scheme 1. Decomposition of CysNO To Produce NO via $Cu_3(BTC)_2$

Table 1. Summary of the Decomposition of CysNO via Cu^{II} Catalysts

conditions	catalyst turnover	time (h)
CysNO:CysH (2:1)	n/a	10.2^b
CysNO:CysH:BTC (2:1:0.66)	n/a	10.2^b
CysNO:CysH:MOF−Cu^{II} (2:1:1)	1.9 ± 0.1^a	10.2 ± 0.2
CysNO:CysH:CuCl$_2$ (2:1:1)	2 ± 0.1^a	0.2 ± 0.1
CysNO:CysH:CuCl$_2$ (2:1:0.0005)	n/a	10.2^b

^{a}Nearly 100% NO recovered. ^{b}Experiment stopped to match the time interval of experiment 3.

The structural rigidity of the framework and the reaction media postreaction were evaluated to further support that the generation of NO was not due to framework instability.

Nitric oxide production was measured directly by chemiluminescence to determine the catalytic turnover of the MOF. Briefly, the MOF was suspended in ethanol containing 1 reducing equivalent of cysteine (CysH). Subsequently, CysNO was added and the real-time production of NO monitored. The addition of 2, 10, and 15-fold excess CysNO to Cu^{II} resulted in the spontaneous generation of NO and nearly 100% theoretical yield of the NO product (see Table 2). In each case $Cu_3(BTC)_2$ had the anticipated turnover with respect to available Cu^{II} centers. In contrast, the absence of the MOF failed to produce a significant amount of NO from a CysNO:CysH solution. These experiments clearly show the ability of the MOF to catalyze the generation of NO from the decomposition of CysNO.

The time release profiles demonstrating the generation of NO are shown in Figure 2. The CysNO decomposition of the MOF-catalyzed reaction was initially more rapid followed by a

Table 2. Catalytic Production of NO via Turnover of the MOF−Cu^{II} Sites

conditions	catalyst turnover^a
CysNO:CysH:MOF−Cu^{II} (2:1:1)	1.9 ± 0.1
CysNO:CysH:MOF−Cu^{II} (10:1:1)	9.8 ± 0.3
CysNO:CysH:MOF−Cu^{II} (15:1:1)	15.0 ± 0.1
CysNO:CysH:MOF−Cu^{II} Recycling	8.0 ± 0.3

^{a}Nearly 100% NO recovered; see SI.
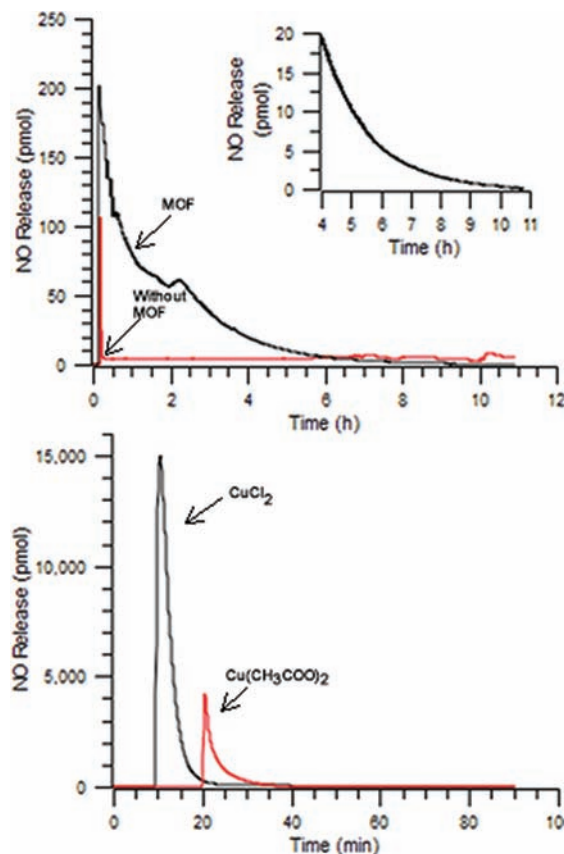
Figure 2. (A) NO release profile of CysNO catalyzed with and without $Cu_3(BTC)_2$. The inset shows an enlargement of the 4−11 h time period for CysNO decomposition by $Cu_3(BTC)_2$. (B) NO release profile of CysNO (black) catalyzed by $Cu(CH_3COO)_2$ and (red) CuCl$_2$.

slower rate of decomposition (Figure 2A). The initial bolus of NO release can be attributed to equilibration of CysNO in the reaction medium. The slight increase in the NO release profile after 2 h may be attributed to an increased availability of the MOF−Cu^{II} sites as a result of the formation of disulfide products. This behavior was found reproducibly after a total of 50% of the CysNO had decomposed. However, in the absence of a catalyst there were no deviations in the NO release profiles over the course of the experiment. In contrast, the addition of GSNO to the MOF did not produce appreciable NO as compared to the CysNO which quantitatively decomposed to produce NO (see SI). The lack of NO production from GSNO may be attributed to the size of the GSNO compared to the size of the pore cavity in $Cu_3(BTC)_2$. The overall size of the cavity is 18 Å. Since the size of GSNO is 19 Å, the access of the GSNO to an active Cu^{II} site is limited.

To demonstrate if the MOF could function as a catalyst for continued use, recycling experiments were performed. After the

CysNO had completely decomposed, the MOF catalyst was removed from the reaction flask, rinsed, and subsequently reacted with 2 additional equivalents of CysNO for three iterations. After each successive addition of CysNO/CysH, the catalyst remained active. This was evident by the consistent turnover of the MOF−Cu^{II} sites as a function of reusing the MOF material (Table 2).

As a comparison to verify that the observed NO generation was due to the MOF and not Cu^{2+} ions in solution, similar NO generation experiments were performed using CuCl$_2$ and Cu(CH$_3$COO)$_2$ as catalysts. The decomposition of CysNO in the presence of CuCl$_2$ was 50 times faster than that of the MOF-catalyzed system, shown in Figure 2B. When Cu-(CH$_3$COO)$_2$ was evaluated as a catalyst for the decomposition of CysNO, the immediate release of NO was observed. NO release was sustained for a 1 h period resulting in 80 ± 5% of the theoretical NO accounted for. In comparison to Cu$_3$(BTC)$_2$ the resulting profiles were markedly different, indicating that the conversion of CysNO to NO is occurring as a function of the MOF structure and not the solvated Cu^{2+} ion species in solution. The slowed rate of reaction by the Cu$_3$(BTC)$_2$ is attributed to the accessibility of the active sites within the MOF network. Given the small interior pore space (18 Å), occupation of a pore is restricted to only one CysNO at a time. This accounts for the slowed rate of reaction in comparison to solvated copper salts which are freely accessible to CysNO. Since the ratio and concentrations of CysNO to Cys to Cu^{II} were held constant, the slower reaction rate of the Cu^{II}−MOF system compared to that of CuCl$_2$ strongly suggests that decomposition of the CysNO is mediated by the MOF instead of any nonframework Cu^{2+} complexes that may be present in the solution.

To further substantiate that the CysNO decomposition was not mediated by nonframework Cu^{2+} complexes, the MOF particles were filtered from the solution. Both the filtrate and the recovered MOF particles were then extensively characterized. The filtrate was evaluated for copper content using ICP-OES via EPA method 200.8.[11] The residual copper in the solution was found to be 0.1 ± 0.08% of the total MOF copper content. Previous work by Poppl has shown that Cu$_3$(BTC)$_2$ contains nonframework Cu^{2+} complexes within the MOF pore space which may account for the solution copper content.[12]

The contribution of the solution Cu^{2+} content toward the overall NO generation was determined by adding an appropriate aliquot of CuCl$_2$ to a solution of CysNO/CysH. The resulting NO generation was similar to that of the control CysNO/Cys experiments and is shown in the Supporting Information [SI] as Figure S8. This result indicates that the nonframework Cu^{2+} in solution does not contribute to the overall decomposition of CysNO.

The filtered MOF particles were examined via pXRD and ATR-IR to provide insights into the structural robustness of the MOF following reaction with CysNO/CysH. Upon desolvation, the MOF particles underwent the expected characteristic color change from turquoise to dark purple. Furthermore, the reacted particles were evaluated for changes in crystallinity by powder X-ray diffraction (pXRD). A direct comparison of the powder patterns of the fresh catalyst and the reacted material suggest that the crystallinty of the framework remained unaltered as shown in Figure 3. This is evident by the identical reflexions and the anticipated 2d line spacings. Further support that the original structure was maintained was evidenced in the ATR-IR spectra. No deviations in the IR resonances were
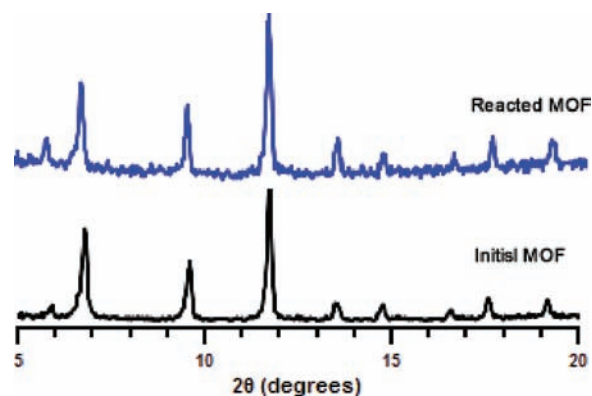
Figure 3. Powder diffraction patterns of Cu$_3$(BTC)$_2$ after reaction of CysNO/CysH (top) and Cu$_3$(BTC)$_2$ before reaction with CysNO/CysH (bottom).

observed between the fresh and reacted particles (see Figure S3 in the SI). Taken together, these data indicate that the MOF catalyst remains structurally robust during and after the reaction.

In summary, the use of a MOF as an NO catalyst is a significant step toward developing advanced NO materials for longer delivery times. In contrast to NO donors, these materials have the potential to overcome the inherent loading capacities of NO donors. This work clearly demonstrates that MOFs can be used as catalysts in the decomposition of RSNOs. This is the first time that a MOF has been used to catalytically decompose RSNO to produce the therapeutic NO species. Although these materials have a high copper content per unit mass, the amount of MOF needed to produce NO at physiologically relevant levels is below the recommended daily dose of copper. Thus, MOFs present an ideal candidate material to ultimately produce NO in vivo from biologically available sources without resulting in toxicity issues. Future studies aim to take advantage of this catalytic activity by developing catalysts that are hydrolytically robust in aqueous solution and that can be formulated for the site-specific generation of NO to control a range of cellular responses.

■ ASSOCIATED CONTENT

Ⓢ Supporting Information

Experimental procedures, NO release profiles of RSNOs by various catalysts, and the IR spectra of Cu$_3$(BTC)$_2$ after reaction with RSNOs and the disulfide product. This material is available free of charge via the Internet at http://pubs.acs.org.

■ AUTHOR INFORMATION

Corresponding Author

melissa.reynolds@colostate.edu

Notes

The authors declare no competing financial interest.

■ ACKNOWLEDGMENTS

■ REFERENCES

(1) (a) Palmer, R. M. J.; Ferrige, A. G.; Moncada, S. *Nature* **1987**, *327*, 524. (b) Marletta, M. A. *Trends Biochem. Sci.* **1989**, *14*, 488. (c) Bogdan, C. *Nat. Immunol.* **2001**, *2*, 907.

(2) (a) Frost, M. C.; Reynolds, M. M.; Meyerhoff, M. E. *Biomaterials* **2005**, *26*, 1685. (b) de Mel, A.; Murad, F.; Seifalian, A. M. *Chem. Rev.* **2011**, *111*, 5742. (c) Seabra, A. B.; Duran, N. *J. Mater. Chem.* **2010**, *20*, 1624.

(3) (a) Reynolds, M. M.; Hrabie, J. A.; Oh, B. K.; Politis, J. K.; Citro, M. L.; Keefer, L. K.; Meyerhoff, M. E. *Biomacromolecules* **2006**, *7*, 987. (b) Coneski, P. N.; Nash, J. A.; Schoenfisch, M. H. *ACS Appl. Mater. Interfaces* **2011**, *3*, 426.

(4) (a) Shin, J. H.; Metzger, S. K.; Schoenfisch, M. H. *J. Am. Chem. Soc.* **2007**, *129*, 4612. (b) Liu, H. A.; Balkus, K. J. *Chem. Mater.* **2009**, *21*, 5032.

(5) Hinks, N. J.; Mckinlay, A. C.; Xiao, B.; Wheatley, P. S.; Morris, R. E. *Microporous Mesoporous Mater.* **2010**, *129*, 330.

(6) (a) Xiao, B.; Wheatley, P. S.; Zhao, X.; Fletcher, A. J.; Fox, S.; Rossi, A. G.; Megson, I. L.; Bordiga, S.; Regli, L.; Thomas, K. M.; Morris, R. E. *J. Am. Chem. Soc.* **2007**, *129*, 1203. (b) Ingleson, M. J.; Heck, R.; Gould, J. A.; Rosseinsky, M. J. *Inorg. Chem.* **2009**, *48*, 9986. (c) Nguyen, J. G.; Tanabe, K. K.; Cohen, S. M. *CrystEngComm* **2010**, *12*, 2335. (d) Wheatley, P. S.; Butler, A. R.; Crane, M. S. *J. Am. Chem. Soc.* **2006**, *128*, 502. (e) Boes, A; Wheatley, P. S.; Xiao, B.; Megson, I. L.; Morris, R. E. *Chem. Commun.* **2008**, *46*, 6146. (f) Boes, A.; Xiao, B.; Megson, I. L.; Morris, R. E. *Top. Catal.* **2009**, *52*, 35−41.

(7) (a) Williams, L. H. *Acc. Chem. Res.* **1999**, *32*, 869. (b) Askew, S. C.; Barnett, D. J.; McAninly, J.; Williams, D. L. H. *J. Chem. Soc., Perkin Trans. 2* **1995**, *8*, 741.

(8) Chui, S.; Lo, S. M.; Charmant, J. P. H; Orpen, A. G.; Williams, I. D. *Science* **1999**, *283*, 1149.

(9) Corma, A.; García, H.; Llabrés i Xamena, F. X. *Chem. Rev.* **2010**, *110*, 4606.

(10) Thomas, D. D.; Flores-Santana, W.; Switzer, C. H. ; Wink, D. A.; Ridnour, L. A. Determinants of Nitric Oxide Chemistry: Impact of Cell Signaling Processes. In *Nitric Oxide:Biology and Pathology*; Ignarro, L. J., Ed.; Elsevier: New York, NY, 2010;993−27.

(11) Long, S. E., Martin, T. D., Martin, E. R. Determination of Trace Elements in Waters and Wastes by Inductively Coupled Plasma-Mass Spectrometry, *Method 200.8*; Environmental Protection Agency; Environmental Monitoring Systems Laboratory Office of Research and Development: Cincinnati, OH, 1994.

(12) Poppl, A.; Kunz, S.; Himsl, D.; Hartmann, M. *J. Phys. Chem. C* **2008**, *112*, 2678.